Research Article | Vol. 26, No. 4 | 19 Feb 2018 | OPTICS EXPRESS 4942
Optics EXPRESS

Transmission analysis for OFDM signals over hybrid RF-optical high-throughput satellite

DIMITAR R. KOLEV* **AND MORIO TOYOSHIMA**

Space Communications Laboratory, National Institute of Information and Communications Technology (NICT), Japan
*dkolev@nict.go.jp

Abstract: In this paper, a theoretical investigation of the performance of a communication scenario where a geostationary-orbit satellite provides radio-frequency broadband access to the users through orthogonal-frequency-division multiplexing technology and has an optical feeder link is presented. The interface between the radio frequency and the optical parts is achieved by using radio-on-fiber technology for optical-electro and electro-optical conversion onboard and no further signal processing is required. The proposed scheme has significant potential, but presents limitations related to the noise. The noise in both forward and reverse links is described, and the system performance for an example scenario with 1280 MHz bandwidth for QPSK, 16QAM, and 64QAM subcarrier modulation is estimated. The obtained results show that under certain conditions regarding link budget and components choice, the proposed solution is feasible.

OCIS codes: (060.2605) Free-space optical communication; (010.1300) Atmospheric propagation.

References and links

1. M. Toyoshima, K. Takizawa, T. Kuri, W. Klaus, M. Toyoda, H. Kunimori, T. Jono, Y. Takayama, M. Mokuno, and K. Arai, "Results of Ground-to-Space Optical Communications Experiments using a Low Earth Orbit Satellite," *19th Annual Meeting of the IEEE Lasers and Electro-Optics Society* (2006), pp.80–81.
2. B. V. Oaida, M. J. Abrahamson, R. J. Witoff, J. N. B. Martinez, and D. A. Zayas, "OPALS: An optical communications technology demonstration from the International Space Station," *2013 IEEE Aerospace Conference* (2013), pp.1–20.
3. D. Giggenbach, J. Horwath, and B. Epple, "Optical Satellite Downlinks to Optical Ground Stations and High-Altitude Platforms," *16th IST Mobile and Wireless Communications Summit* (2007), pp. 1–4.
4. Y. Koyama, M. Toyoshima, Y. Takayama, H. Takenaka, K. Shiratama, I. Mase, and O. Kawamoto, "SOTA: Small Optical Transponder for micro-satellite," *2011 International Conference on Space Optical Systems and Applications* (2011), pp. 97–101.
5. F. Heine, H. Kämpfner, R. Czichy, R. Meyer, and M. Lutzer, "Optical inter-satellite communication operational," *2010 Military Communications Conference* (2010), pp. 1583–1587.
6. K. Suzuki, M. Yahata, M. Kato, T. Watanabe, K. Hoshi, T. Okui, S. Yoshikawa, M. Yoneda, Y. Arakawa, T. Asai, T. Takahashi, and M. Toyoshima, "16APSK/16QAM-OFDM 3.2Gbps RF Signal Direct-Processing Transmitter and Receiver Communication Experiment Using WINDS Satellite," *IEICE Technical Report SAT2015–40 (2015–10)*, pp. 137–140.
7. B. Roy, S. Poulenard, S. Dimitrov, R. Barrios, D. Giggenbach, A. L. Kernec, and M. Sotom, "Optical feeder links for high throughput satellites," *2015 IEEE International Conference on Space Optical Systems and Applications* (2015), pp. 1–6.
8. S. Dimitrov, B. Matuz, G. Liva, R. Barrios, R. Mata-Calvo, and D. Giggenbach, "Digital modulation and coding for satellite optical feeder links," *2014 7th Advanced Satellite Multimedia Systems Conference and the 13th Signal Processing for Space Communications Workshop (ASMS/SPSC)* (2014), pp. 150–157.
9. L. C. Andrews and R. L. Phillips, *Laser Beam Propagation Through Random Media* (SPIE Press, 2005).
10. P. T. Dat, A. Bekkali, K. Kazaura, K. Wakamori, and M. Matsumoto, "A universal platform for ubiquitous wireless communications using radio over FSO system," J. Lightwave Technol. **28**(16), 2258–2267 (2010).
11. C. Petit, N. Védrenne, M. Velluet, V. Michau, G. Artaud, E. Samain, and M. Toyoshima, "Investigation on adaptive optics performance from propagation channel characterization with the small optical transponder," Opt. Eng. **55**(11), 111611 (2016).
12. M. W. Wright, J. F. Morris, J. M. Kovalik, K. S. Andrews, M. J. Abrahamson, and A. Biswas, "Adaptive optics correction into single mode fiber for a low Earth orbiting space to ground optical communication link using the OPALS downlink," Opt. Express **23**(26), 33705–33712 (2015).
13. Y. Dikmelik and F. M. Davidson, "Fiber-coupling efficiency for free-space optical communication through atmospheric turbulence," Appl. Opt. **44**(23), 4946–4952 (2005).

#303906 https://doi.org/10.1364/OE.26.004942
Journal © 2018 Received 4 Aug 2017; revised 25 Jan 2018; accepted 9 Feb 2018; published 16 Feb 2018

Optics EXPRESS

14. W. Rosenkranz, A. Ali, and J. Leibrich, "Design considerations and performance comparison of high-order modulation formats using OFDM," *2010 12th International Conference on Transparent Optical Networks*, (2010), pp. 1–4.
15. D. R. Kolev, K. Wakamori, and M. Matsumoto, "Transmission Analysis of OFDM-Based Services Over Line-of-Sight Indoor Infrared Laser Wireless Links," J. Lightwave Technol. **30**(3), 3727–3735 (2012).
16. A. Bekkali, C. B. Naila, K. Kazaura, K. Wakamori, and M. Matsumoto, "Transmission analysis of OFDM-basedwireless services over turbulent radio-on-FSO links modeled by gamma-gammadistribution," IEEE Photonics J. **2**(3), 510–520 (2010).
17. H. Al-Raweshidy and S. Komaki, *Radio Over Fiber Technologies for Mobile Communications Networks* (Artech House, 2002).
18. R. J. Westcott, "Investigation of multiple f.m./f.d.m. carriers through a satellite t.w.t. operating near to saturation," Proc. Inst. Electr. Eng. **114**(6), 726–740 (1967).
19. L. C. Andrews, R. L. Phillips, and C. Y. Hopen, *Laser Beam Scintillation with Applications* (SPIE Press, 2001).
20. D. M. Baney, P. Gallion, and R. S. Tucker, "Theory and measurement techniques for the noise figure of optical amplifiers," Opt. Fiber Technol. **6**(2), 122–154 (2000).
21. J. H. Churnside, "Aperture averaging of optical scintillations in the turbulent atmosphere," Appl. Opt. **30**(15), 1982–1994 (1991).
22. J. Li, Y.-C. Zhang, S. Yu, T. Jiang, Q. Xie, and W. Gu, "Intermodulation distortion elimination for analog photonics link based on integrated dual-parallel Mach-Zehnder modulator," in *CLEO 2014* (2014).
23. R. J. Alliss and B. Felton. "Realtime atmospheric decision aids in support of the lunar laser communications demonstration," in *Proceedings of the International Conference on Space Optical Systems and Applications* (ICSOS, 2014).

1. Introduction

Recently, satellite laser communication technology is gaining popularity by offering reduced system size, weight, and power (SWaP) as well as a wider bandwidth [1–4]. Together with the significant benefits of the technology though, there are a few drawbacks that limit its implementation to a number of applications. The biggest challenge remains to be the laser beam propagation through the atmosphere that is strongly influenced by the atmospheric turbulence effects and the clouds. Different solutions, such as site diversity, have been considered in order to increase the link availability to the levels of the RF alternatives. Currently, most suitable applications of the technology are high-speed inter-satellite links where atmosphere is absent [5], and LEO-to-ground links that allow small observation satellites to download significant amount of data during a few-minutes pass [4]. The dominating satellite-to-ground/maritime/aircraft broadband access technology is more likely to continue to be based on radio-frequency (RF), especially with the implementation of the Ka-band [6]. However, there are particular scenarios that consider optical feeder link in a GEO satellite [7]. Of high interest is the development of a system with broadband RF access between the user and the satellite that can be based on a GEO satellite with multiple beams in Ka band [6]. In order to release more RF bandwidth to be used for different applications and/or higher data rates, an optical feeder link that is to be used as a backhaul link between the satellite and the fixed base station on the ground is considered. For such high throughput satellites (HTS), employing both RF and optical technologies of critical importance is the RF-optical interface solution.

First, it is possible to use the RF signal as an input for the optical signal modulation (analog signal transmission on the optical channel, known as radio over fiber (RoF)). Such solution is preferred since it will guarantee satellite transparency regardless of the RF modulation. However, according to the signal, the signal-to-noise ratio (SNR) requirements drastically change and the GEO-GND link is often hard to achieve. Using OFDM modulation with multiple slow rate channels may significantly ease the link requirements.

Second, it is possible to sample the analog RF signal and turn it into a digital one with Analog-Digital Converter (ADC). Such solution requires some special devices, such as high-speed ADC and DAC. Also, it would require significant optical bandwidth to transport the RF signal, which is quite inefficient. For example, the bit stream after the ADC will be increased significantly (e.g. for an 8-bit ADC is expected to have 8 times higher data rate and most likely higher order ADC and at least double sampling speed will be necessary. If a 3.2 Gbps

Optics EXPRESS

RF data rate as in [6] is considered, the required optical downlink is in the order of 20-30 Gbps and that is extremely hard to implement considering the onboard electronics and the link budget limitations, which forms a bottle neck).

Third, it is possible to process the RF signal onboard by using Field Programmable Gate Array (FPGA) or dedicated Integrated Circuit (IC) and transmit it on the optical channel as proposed in [8]. While this method guarantees highest efficiency in terms of used bandwidth and SNR, it requires significant processing power onboard and this would actually form a bottleneck considering the state of the art for onboard equipment.

Following the discussion above, the chosen implementation is based on OFDM as simplest and probably with best performance when HTS with RF-Optical interface are discussed. Of utmost importance in this work is the configuration that implements radio over fiber (RoF) technologies, particularly the Direct Detection Orthogonal Frequency Division Multiplexing (DD-OFDM) technology by feeding the RF signal to a laser diode (LD) or optical modulator (typically Mach-Zehnder Modulator (MZM)) that can convert the RF signal to an optical one and send through an optical channel. For the optical to RF signal conversion, the photodiode (PD) itself converts the received optical power to an electrical (RF) signal. The proposed scenario has a lot of limitations, especially considering the noise in the links. However, it allows for seamless transmission of the data. Furthermore, OFDM is considered instead of Time Division Multiplexing (TDM) so that no further processing at the satellite is to take place and the lower data rates in each subcarrier that are robust to higher levels of noise. However, OFDM implementations are sensitive to Doppler shift and a proper compensation is required. The effect in GEO to ground links is much smaller compared to LEO-to-ground links.

This paper is divided as follows. In Section 2, the hybrid forward (optical uplink from the gateway to the satellite and RF downlink to the user) and return (RF uplink from the user to the satellite and optical downlink to gateway) link are described in detail with the different kinds of noise, present in the channels, including the intermodulation distortion and the scintillation. In Section 3, the theory from Section 2 is implemented into a real system design example to estimate the performance. Finally, the paper concludes in Section 4.

2. Proposed system design and theoretical model

The considered high-throughput satellite scenario is shown in Fig. 1. The user access remains RF-based while the link between the ground base station and the satellite is optical.

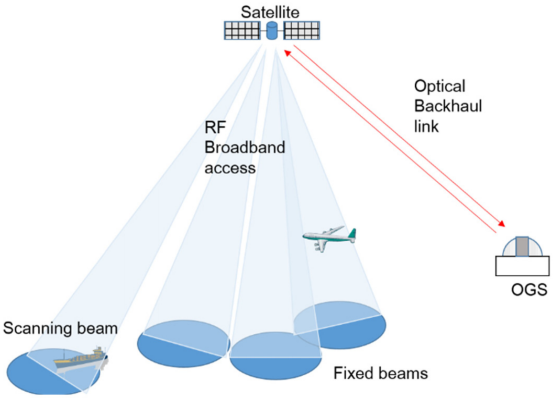

Fig. 1. High-throughput satellite with optical feeder link.

2.1 Optical link budget

While RF technology and particularly Ka-band are widely studied and used in satellite communications, laser communications technology is relatively novel and still developing

Optics EXPRESS

technology with different issues to be considered [1–4]. Therefore, in the presented analysis the RF links are not described in terms of link budget, but only consider the Carrier to Noise Ratio (CNR) degradation due to the RF Low Noise Amplifiers noise figures and the main accent is on the laser links.

In Table 1, the link budget for both optical uplink and downlink in the case of a GEO satellite is shown. The results are similar to [8], with some important differences.

Optical transmit power in satellite communications is a critical parameter- there are power limitations in the uplink due to eye safety and in the downlink due to the available onboard power. It is important to decrease the power as much as possible, and for this reason a 10 W laser in the uplink and 5 W laser in the downlink have been chosen, which is significantly lower compared to the 50-Watt uplink and 10-Watt downlink optical powers, considered in [8]. For different implementation scenarios, some parameters could drastically change thus allowing further decreasing of the transmit power levels but a more general case has been addressed in this paper.

Table 1. Link Budget for the Uplink and the Downlink of the Optical Channel

	Notation	Uplink	Downlink	
Tx Power	P_{OTX}	40	37	dBm
Tx optics loss	L_{OTX}	−2	−2	dB
Tx Antenna Diameter	D_{OTX}	0.2	0.2	m
Beam waist	ω_0	0.130	0.130	m
Wavelength	λ	1550	1550	nm
Distance	R	38000	38000	km
Beam angle of divergence	θ_0	15.2	15.2	μrad
Tx Antenna Gain	G_{OTX}	111.4	111.4	dB
Losses (pointing, atmospheric attenuation, etc.)	L_{OLink}	−6	−6	dB
Geometric loss	L_{geom}	−289.8	−289.8	dB
Rx Antenna gain	G_{ORX}	112.2	112.2	dB
Rx optics loss	L_{ORX}	−3	−3	dB
Atm. Turbulence loss	L_{scint}	−10	−10	dB
Rx Antenna diameter	D_{ORX}	0.2	0.2	m
Additional gain	G_{add}	0	10	dB
Sat. OA gain	G_{OA}	12	12	dB
Rx power in PD	P_{ORX}	−35.2	−28.2	dBm

For simplicity some of the losses have been combined (e.g. pointing loss, atmospheric loss, etc.). Onboard the satellite, it is better to have a lower transmit power in order to save resources. The transmit optical power is chosen to be 5 W instead of 10 W, and if the link budget allows, it is highly recommended to decrease further.

There are three possible ways to receive the optical signal –directly concentrating the power over an avalanche photodiode (APD) or similar, coupling the signal into a multimode fiber and later coupling it again to a photodiode, or coupling the signal into a single mode fiber. Due to the atmospheric turbulence [9], the angle of arrival is constantly changing, which leads to beam wandering in the focal plane. One solution is to use a PD with very big size, but due to its capacitance there will be a severe limitation in its bandwidth. Coupling to a multimode fiber is relatively easy considering its big size (around 200 micrometer diameter core), compared to a single mode fiber (below 10 micrometer diameter core). To facilitate the coupling for all the methods, there are several technologies including tip/tilt correction that can compensate relatively fast the beam wandering [10], and adaptive optics (AO [11, 12]) correction, that is widely used in astronomy to correct the beam wavefront aberrations after propagating through the turbulent atmosphere. For this purpose, a row called “Additional gain” was added to bring 0 dB gain in the uplink, but if an AO system is installed in the optical ground station (OGS), that could add a gain of 7 dB [11], or even over 10 dB in the downlink [12]. Such possibility has not been considered in [8]. In this proposal, RoF technology is used. If single mode fiber coupling is required, such coupling of an optical signal after propagation through the atmosphere leads to very high losses L_{scint} [13] and OA is

Optics EXPRESS

necessary before the PD. To leave space for further link improvement and for easier comparison with direct PD receiver without coupling, the OA gain G_{OA} is set to be equal to the losses due to fiber coupling. Thus, the received optical power in the PD is equal regardless if fiber coupling is used or not.

The provided notations in Table 1 are with capital letters, denoting that the values are in dB/dBm for easier link budget calculation. However, in the following noise analysis the same notations with small letters denote values, used as coefficients for easier noise calculation.

2.2 Forward link

The forward link scenario is shown in Fig. 2. At the OGS, the signal is being encoded and interleaved for higher resistance to the signal fading due to atmospheric turbulence [9]. Then the signal goes to an OFDM transmitter. The considered subcarrier modulation types are m-QAM. The output of the OFDM transmitter is taken directly to a LD or a MZM to modulate the optical signal, as often implemented in RoF technology [14]. The optical power output from the LD will be [15–17]:

$$p_{MZM}(\mathrm{t}) = p_t\left(1+\sum_{n=0}^{N-1} m_n s_n(\mathrm{t}) + a_3\left[\sum_{n=0}^{N-1} m_n s_n(\mathrm{t})\right]^3\right). \quad (1)$$

where p_t is the average transmitted optical power, a_3 is the third order nonlinearity coefficient, $m_n = m/\sqrt{N}$ is the optical modulation index (OMI) for the n-th subcarrier (m is the total OMI) assuming that all tones are to be modulated with the same modulation index m_n, and s(t) is the signal at the n-th sub-carrier.

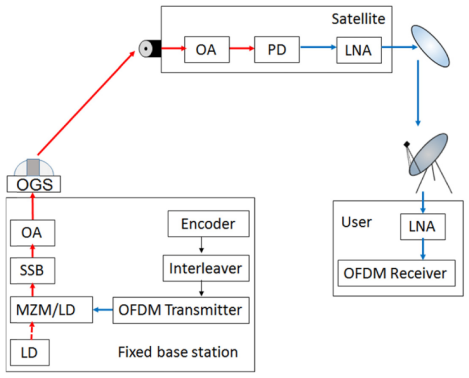

Fig. 2. Forward link block scheme.

The received optical power in the satellite photodetector will be:

$$p_{ORX} = p_{OTX} g_{OTX} l_{OLink} l_{geom} g_{ORX} l_{ORX} l_{sc\,int} g_{add} g_{OA,Sat} X + n_{FSO}(\mathrm{t}). \quad (2)$$

where X quantifies the variation of the signal fading due to atmospheric turbulence transmission effects and its probability density function (PDF) is often defined to be Gamma-Gamma [9], and n_{FSO} characterizes the additive white Gaussian noise (AWGN) and is assumed that it can be filtered in the PD and is not consider in the further analysis. If direct fiber coupling is implemented, due to the angle of arrival change and the wavefront aberrations the beam could not be inserted in the single mode fiber efficiently and losses l_{scint} will be added. After coupling, however, an optical amplifier with gain g_{OA} can be added to amplify the optical signal prior to PD direct detection.

The nonlinearity in the LD and MZM will lead to increased noise mainly due to the third order modulation distortion (IMD3), since these components lie very close to the fundamental

Optics EXPRESS

carriers and cannot be easily removed by RF filtering [15–17]. The IMD3 which falls into the *n*-th subcarrier among equally spaced *N* carriers can be described as [15–17]:

$$\sigma_{IMD}^2 = 0.5(0.75\,a_3 m_n^3 D_2 + 1.5\,a_3 m_n^3 D_3)^2 I_{ORX}^2 \cdot \\ I_{ORX} = \rho P_{ORX} \tag{3}$$

where I_{ORX} is the current at the photodiode in the satellite, ρ is the photodiode responsitivity, and D_2 and D_3 represent the number of intermodulation distortion products, which influence the desired carrier. As described in [17, 18], if the number of subcarriers is over six, D_2 can be neglected. Furthermore, for high number of transmitted carriers, the maximum number of intermodulation products is generated in the center of the band ($n = N/2$) and [17, 18]:

$$D_3\Big|_{n=N/2}^{n\to\infty} = 0.75N^2 \\ D_3\Big|_{n=1,N}^{n\to\infty} = 0.25N^2. \tag{4}$$

Another important noise to be considered for analog transmission is the relative intensity noise of the laser diode (RIN) γ_{RIN}. Typical values are in the order of −130~-160 dB/Hz.

The desired signal power in the PD can be expressed as

$$C = 0.5m^2 I_{ORX}^2. \tag{5}$$

Considering the losses in the OGS and the required levels for the optical uplink budget, an optical amplifier (OA) with very high gain is necessary in the optical ground station. Such gain will affect not only the signal but also the noise, adding additional noise due to the amplified spontaneous emission in the amplifier (ASE noise). Similar to the electronic amplifiers, the concept of noise figure can be applied to OA [19], where the noise figure represents the SNR degradation between the input and the output signals of the optical amplifier, and includes the ASE noise. Therefore, the OA noise figure is used in the following analysis instead of the ASE noise itself. The parameter nf_{TXOA} is defined to be the noise figure of the OA in the OGS, and nf_{RXOA} to be the noise figure of the OA in the satellite side. Small letters are used to emphasize that the noise figure values are not in dB thus $CNR_{in} = nf^*CNR_{out}$.

Including the thermal and shot noise in the receiver, the total noise in the PD will be:

$$N_{tot,Opt} = \frac{\frac{4K_B T_{abs}}{R_L} + 2qI_{ORX}}{T_s} + \left(\frac{(\mathrm{RIN})\,I_{ORX}^2}{T_s} + \sigma_{IMD}^2\right)\mathrm{nf}_{TXOA}\, nf_{RXOA}. \tag{6}$$

where, K_B is the Boltzmann's constant, T_{abs} is the absolute temperature, q is the electron charge and T_s is the OFDM symbol duration. The guard interval is set to zero and thus T_s equals to the Fourier analysis window. From here, the carrier to noise and distortion ratio for the *n*-th sub-carrier $CNDR_{n\_ORX} = C/N_{tot}$ can be derived by using Eqs. (5) and (6).

The PD current is directly amplified and sent through the satellite RF antenna with no further processing. When received in the ground antenna, the signal is amplified and sent to the OFDM receiver. $CNDR_{FWD}$ will be further decreased because of the noise figures of the RF low noise amplifiers in the satellite and in the user side – nf_{TXLNA} and nf_{RXLNA}.

$$N_{tot,\mathrm{FWD}} = N_{tot,Opt} nf_{TXLNA} nf_{RXLNA}. \tag{7}$$

2.3 Reverse link

In the reverse link (Fig. 3) the user ground-to-satellite link is RF-based and it is assumed that the only noise is the thermal noise that will be further increased by the two OA noise figures (nf_{TXLNA} and nf_{RXLNA}). The received RF signal is directly used to modulate the LD or MZM

Optics EXPRESS

output and the RIN noise and the third order modulation distortion will be added. At the base station side, the noise on the LD output will be further degraded by the noise figures of the OA in the optical downlink (both on the satellite and on the ground) and the shot noise of the receiver will be added. The total noise for the reverse link will be:

$$N_{tot,\mathrm{RVS}} = \left(\frac{4K_B T_{abs}}{R_L} nf_{TXLNA} nf_{RXLNA} + \frac{(\mathrm{RIN})\,\mathrm{I}_{ORX}^2}{T_s} + \sigma_{IMD}^2 \right) \mathrm{nf}_{TXOA}\, nf_{RXOA} + \frac{2qI_{ORX}}{T_s}. \quad (8)$$

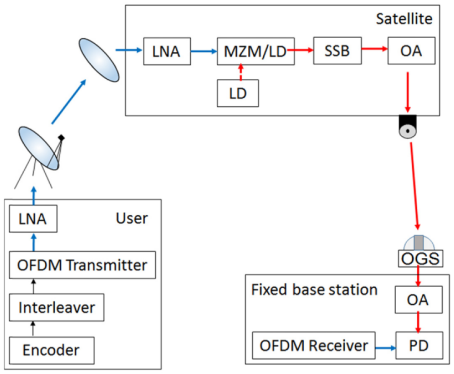

Fig. 3. Reverse link block scheme.

2.4 Symbol and bit error probability (SEP, BEP)

The SEP per subcarrier $P_{s,n}$ for the received M-QAM OFDM signal, where $M = 2^k$ and k is even number, is given by [15, 16]:

$$P_{s,n}(\mathrm{X}) = 2\left(1 - \frac{1}{\sqrt{M}}\right) \mathrm{erfc}\left(\sqrt{\frac{3}{2(\mathrm{M}-1)} CNDR_n(\mathrm{X})}\right). \quad (9)$$

Gamma-Gamma model is often used to describe the signal fluctuations X in the FSO channels and its PDF is:

$$PDF_{\Gamma-\Gamma}(\mathrm{x}) = \frac{2(\alpha\beta)^{\frac{\alpha+\beta}{2}}}{\Gamma(\alpha)\Gamma(\beta)} x^{\frac{\alpha+\beta}{2}-1} K_{\alpha-\beta}\left(2\sqrt{\alpha\beta x}\right). \quad (10)$$

where $\Gamma(.)$ is the Gamma function, $K_n(.)$ is the modified Bessel function of the second kind, α and β are the effective numbers of small scale and large scale eddies and are given with [9]:

$$\alpha = \left[\exp\left\{ \frac{0.49\sigma_R^2}{\left(1+1.11\sigma_R^{12/5}\right)^{7/6}} \right\} - 1 \right]^{-1}$$
$$\beta = \left[\exp\left\{ \frac{0.51\sigma_R^2}{\left(1+0.69\sigma_R^{12/5}\right)^{5/6}} \right\} - 1 \right]^{-1}. \quad (11)$$

where σ_R^2 is the Rytov variance [20]. By using a bigger receiver aperture, aperture averaging effect that leads to lower scintillation index values is observed [20, 21]. That improves the BEP performance of the system, as shown in the next Section.

Following the analysis in [16], the final formula for SEP when Gamma-Gamma PDF is considered for the fading due to scintillation can be provided but instead of the noise in [16],

Optics EXPRESS

Eq. (10), the corresponding CNDR for the forward and reverse links based on the noise Eqs. (7) and (8) is included:

$$\left\langle P_{s,n}\right\rangle = \left(1-\frac{1}{\sqrt{M}}\right)\frac{2^{\alpha+\beta-1}}{\pi\sqrt{\pi}\Gamma(\alpha)\Gamma(\beta)}G_{5,2}^{2,4}\left(\frac{2^3 3CNDR}{2(M-1)(\alpha\beta)^2}\middle|\begin{matrix}\frac{1-\alpha}{2},\frac{2-\alpha}{2},\frac{1-\beta}{2},\frac{2-\beta}{2},1\\ 0,0.5\end{matrix}\right). \tag{12}$$

where $G_{c,d}^{a,b}(.)$ is the MeijerG function.

If Gray-coded mapping is used the average BEP will be [16]:

$$\left\langle P_{b,n}\right\rangle = \frac{1}{\ln(M)}\left\langle P_{s,n}\right\rangle. \tag{13}$$

When the number of subcarriers is large, the total average BEP over the entire OFDM band can be delivered based on the law of large numbers [16]:

$$\left\langle P_b\right\rangle = \frac{1}{N}\sum_{n=0}^{N-1}\left\langle P_{b,n}\right\rangle. \tag{14}$$

3. Results and discussion

For the system characteristics estimation, an OFDM signal that combines multiple 40 MHz WiFi channels with 128 sub-carriers, each with 800 nm guard interval (25%), that results in OFDM symbol duration of 4 μs, was considered. Since the OFDM signal employs IFFT that requires subcarrier number N = 2^n, it is assumed that 32 × 40 MHz channels are covering 1280 MHz bandwidth. As defined by the 802.11n standard for a single spatial stream, the possible M-QAM modulations with the corresponding coding rates and user speeds are shown in Table 2. As mentioned in Section 2, the coding is necessary for error correction mainly due to atmospheric turbulence.

The parameters used in the analysis are listed in Table 3.

Table 2. List of Considered Modulation Types, Coding Rates and Data Rates

Modulation	Coding rate	Data rate (Mbps)	Total user data rate (1.28 GHz bandwidth), Mbps
QPSK	1/2	27	864
QPSK	3/4	40.5	1296
16QAM	1/2	54	1728
16QAM	3/4	81	2592
64QAM	2/3	108	3456
64QAM	3/4	121.5	3888
64QAM	5/6	135	4320

Table 3. Analysis Parameters

Bandwidth	B	1280	MHz
Subcarriers	N	4096	
OFDM symbol duration	T_s	4	μs
Wavelength	λ	1550	nm
Detector responsitivity	ρ	0.85	A/W
Relative intensity noise	RIN	–135	dB/Hz
Absolute temperature	T_{abs}	300	K
PD load resistor	RL	10	kΩ
Third order IMD	a_3	0.0009	

3.1 Optimal CNDR selection

CNDR is dependent mainly on the OMI and the received optical power. In Figs. 4(a) and 4(b), the relationship between CNDR and the OMI and received power respectively for the

Optics EXPRESS

forward and the reverse link are shown. The case of an LD with *RIN = –135* dB/Hz on the transmitter side and fiber coupling and OA in the receiver side was chosen. It can be observed that the strong dependence on the OMI while increasing the received power after a given level leads to no significant improvement. Due to the noise differences, the CNDR in the reverse link is noticeably much higher and it changes much faster.

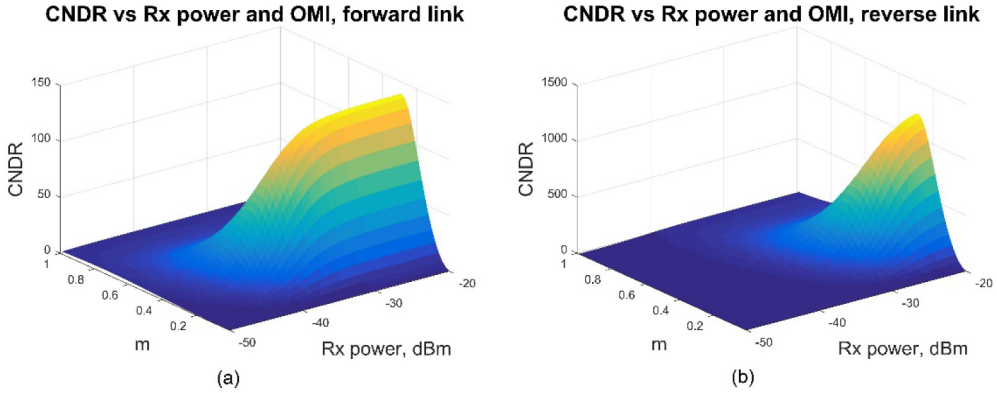

Fig. 4. CNDR vs OMI and received optical power for forward link (a) and reverse link (b).

For optimal OMI that leads to maximal CNDR in both forward and reverse link, the value of 0.29 is chosen and Figs. 5(a) and 5(b) show the relationships between CNDR and the received power for the optimal *OMI = 0.29,* respectively for the forward and reverse link. There are four different cases –LD with *RIN = –135* dB/Hz with fiber coupling or direct PD detection, LD with *RIN = –150* dB/Hz with direct PD detection and MZM with IMD3 and RIN noise reduction through different techniques (e.g. parallel schemes) [22]. For the MZM case, *RIN = –150* dB/Hz and IMD3 is reduced with 20 dB.

The significant effect of lower RIN/IMD3 on the forward link by using MZM instead of LD intensity modulation can be observed. Compared to the scenario with direct fiber coupling and LD with *RIN = –135* dB/Hz, according to the received power using MZM modulator can lead to 15 dB higher CNDR when direct fiber coupling is used and about 20 dB higher CNDR when direct PD detection is used. Also, it can be seen that the removal of the OA when no fiber coupling takes place leads to about 5 dB CNDR improvement. Choosing an LD with lower RIN noise can also significantly improve the CNDR. For example, RIN noise of −150 dB/Hz instead of −135 dB/Hz leads to about 7 dB higher CNDR.

Optics EXPRESS

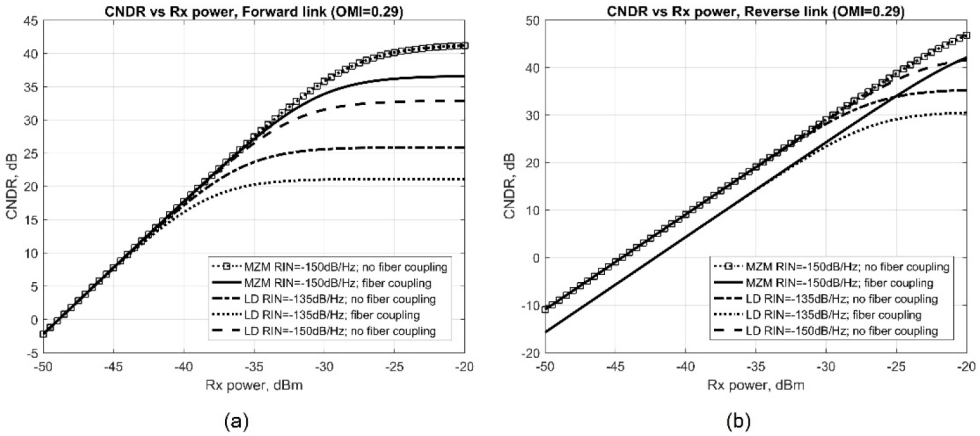

Fig. 5. CNDR vs Rx. Power for optimal OMI for four cases –direct intensity modulation of an LD with and without fiber coupling and different RIN noise and improved modulation with MZM for both forward link (a) and reverse link (b).

While the reverse link CNDR is strongly dependent on the received optical power, it is not significantly affected by the optical modulation type (LD or MZM) and the different parameters of the considered cases. As a general conclusion for lower received power, it is considered that it is better to use a system with no direct fiber coupling since that leads to about 5 dB higher CNDR. It is important to note that the amplifier noise figures would generally be lower than the ones considered (4.77 dB), which will further improve the CNDR.

Further analysis of the effect of the number of channels on the CNDR is performed, since it directly affects the OMI per channel. The results are shown in Table 4. The current choice of 4096 is somehow optimal with 1 dB loss compared to a system with 8192 channels.

Table 4. Number of Channels Analysis

N channels	1024	2048	4096	8192	16384
CNDR_FW, dB	11.15	16.93	21.44	22.21	20.03
CNDR_RS, dB	20.47	26.07	30.42	31.41	29.47

3.2 BEP Analysis

The BEP of the uncoded signal is calculated using Eqs. (12)-(14) for several different cases – no turbulence, weak turbulence and strong turbulence. Considering the aperture averaging effect, the chosen values for the scintillation index for weak turbulence is $\sigma_I^2(\mathrm{D}=0.2\,\mathrm{m})=0.047$ and for strong turbulence is $\sigma_I^2(\mathrm{D}=0.2\,\mathrm{m})=0.316$.

The dependence of BEP on CNDR for QPSK (Fig. 6(a)), 16QAM (Fig. 6(b)) and 64QAM (Fig. 6(c)) is shown for two different scenarios –no turbulence to strong turbulence condition defining a range of possible turbulence conditions.

Assuming BER = 10^{-3} to be enough for errorless transmission of the coded signal, it can be observed that the required CNDR for the proposed system to operate under all atmospheric conditions is 21.8 dB for QPSK, 28.2 dB for 16QAM and 33.8 dB for 64QAM. Considering the CNDR results from Figs. 5(a) and 5(b) and their dependence on the received power, the CNDR for the different cases can be listed in Table 5. The link budget in Table 1 assumes fiber coupling and includes 10 dB coupling loss due to scintillation and 12 dB OA gain. For the cases with no fiber coupling we assume losses due to scintillation of 3 dB and lack of OA gain, which results in 9 dB less received power.

Optics EXPRESS

Table 5. Achieved CNDR for the Different Scenarios

Link	Scenario	CNDR	
Forward	LD, RIN −135dB/Hz, fiber coupling	20.1	dB
	LD, RIN −150dB/Hz, fiber coupling	26.1	dB
	LD, RIN −135dB/Hz, no fiber coupling	9.3	dB
	MZM, RIN −150 dB/Hz, IMD3-20dB, fiber coupling	9.4	dB
	MZM, RIN −150 dB/Hz, IMD3-20dB, no fiber coupling	9.4	dB
Reverse	LD, RIN −135dB/Hz, fiber coupling	26	dB
	LD, RIN −150dB/Hz, fiber coupling	32.2	dB
	LD, RIN −135dB/Hz, no fiber coupling	14.8	dB
	MZM, RIN −150 dB/Hz, IMD3-20dB, fiber coupling	14.8	dB
	MZM, RIN −150 dB/Hz, IMD3-20dB, no fiber coupling	14.8	dB

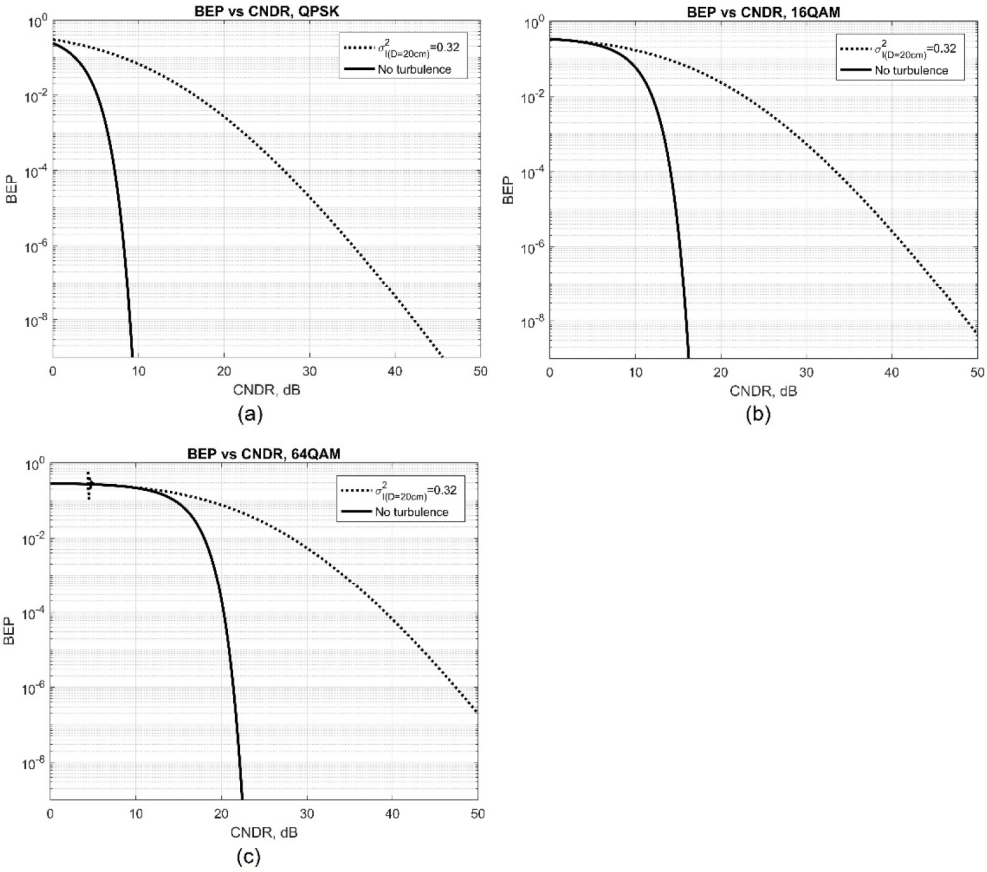

Fig. 6. BEP vs CNDR for QPSK (a), 16QAM (b), and 64QAM (c) signal without turbulence to strong turbulence conditions.

The values in Table 5 show the significant effect of the link budget on the link throughput. Under the proposed link budget only fiber coupling solutions can transport the OFDM signal with different success. Considering the CNDR to received power ratio on Figs. 5(a) and 5(b), there are several solutions to improve the system throughput.

Optics EXPRESS

In the forward link, the transmit power of the OGS can be increased to the levels of [8]. This would secure up to 7 dB higher received power and the CNDR will vary in the order of 21 dB to 37 dB thus allowing 64QAM for the fiber coupling with OA implementations and QPSK for the other cases. However, the implementation of a fiber coupled LD with −135 dB/Hz RIN noise, would not be able to support higher order modulation than QPSK regardless of the received power level. Higher gains (over 30 dB) for the OA are possible and this could significantly relax the system requirements (e.g. OGS transmit power). Another possibility is to increase the receiving aperture size, which would lead to higher levels of received power and stronger aperture averaging effect, resulting in smaller power fluctuations due to turbulence. However, apart from the increased size and weight, such solution would make direct fiber coupling harder increasing the coupling loss. As a conclusion, an optical source with low RIN noise is critical.

In the reverse link, the considered link budget provides CNDR that for the fiber coupling scenarios is enough to transmit 16QAM signal, even under strong turbulence. Nevertheless, the optical downlink provides further possibilities for improvement and 64QAM transmission. Bigger aperture size (typically in the range of 40 cm to 60 cm) would significantly increase the received power level, respectively the system CNDR, and decrease the power fluctuations due to aperture averaging that would further decrease the required CNDR for the desired BEP. Furthermore, AO system could be integrated in the OGS side. The considered AO gain was set to be 12 dB, but much higher gain is possible [12]. All these improvements allow to decrease the satellite OA gain directly leading to a better SWaP or consideration of higher orders of modulation or simpler implementations.

Finally, while feeder link is supposed to be available 24/7, due to the atmospheric conditions (e.g. clouds, rain, sandstorm, etc.) in practice, the availability of satellite to ground laser links is expected to be quite low. As mentioned earlier, site diversity is a typical solution for this problem. The technology relies on the deployment of multiple OGS stations around the Globe with uncorrelated weather conditions and relatively high availability in terms of sunny days/hours per year. Thus, if there is rain at one site, there is high probability that another OGS has clear sky and handover can take place [23]. The handover decisions can be improved to consider not only the weather conditions, but also the seeing parameters (atmospheric turbulence conditions) allowing further improvement of the system.

4. Conclusion

A network with broadband user access to a satellite and an optical feeder link has been presented. Compared to alternative solutions, the proposed design onboard the satellite is very simple and requires no data processing. Both forward and reverse links have been analyzed and the close-form equations for the total noise in the system were provided. Based on the theoretical equations different optical modulation solutions (LD, MZM) of the proposed system have been evaluated for a given OFDM signal and three different subcarrier modulations –QPSK, 16QAM and 64QAM. The results show the design considerations and strict limitations in the forward link and possible solutions to allow higher order modulation schemes to be used. The proposed reverse link allows much easier implementation even under the shown link budget, which allows further design optimization (e.g. lower transmit power on the satellite side). The chosen parameters are not optimal to allow future system performance improvement.

As a general conclusion, while in terms of CNDR versus received power performance the fiber coupling implementations show worse results, the link budget limitations clearly make other choices hard to implement efficiently and in terms of throughput fiber coupling with OA prior to signal detection would be a preferred choice.

This work could be used as a reference for future design of hybrid satellite networks with broadband RF user access network and optical feeder link employing the proposed plain design with no processing onboard.